

Radiolarian faunal turnover through the Paleocene-Eocene transition, Mead Stream, New Zealand

Autor(en): **Hollis, Christopher J.**

Objektyp: **Article**

Zeitschrift: **Eclogae Geologicae Helvetiae**

Band (Jahr): **99 (2006)**

Heft [1]: **Radiolaria : siliceous plankton through time : proceedings of the tenth meeting of the International Association of Radiolarian Palaeontologists INTERRAD X**

PDF erstellt am: **26.09.2024**

Persistenter Link: <https://doi.org/10.5169/seals-169256>

Nutzungsbedingungen

Die ETH-Bibliothek ist Anbieterin der digitalisierten Zeitschriften. Sie besitzt keine Urheberrechte an den Inhalten der Zeitschriften. Die Rechte liegen in der Regel bei den Herausgebern.

Die auf der Plattform e-periodica veröffentlichten Dokumente stehen für nicht-kommerzielle Zwecke in Lehre und Forschung sowie für die private Nutzung frei zur Verfügung. Einzelne Dateien oder Ausdrucke aus diesem Angebot können zusammen mit diesen Nutzungsbedingungen und den korrekten Herkunftsbezeichnungen weitergegeben werden.

Das Veröffentlichen von Bildern in Print- und Online-Publikationen ist nur mit vorheriger Genehmigung der Rechteinhaber erlaubt. Die systematische Speicherung von Teilen des elektronischen Angebots auf anderen Servern bedarf ebenfalls des schriftlichen Einverständnisses der Rechteinhaber.

Haftungsausschluss

Alle Angaben erfolgen ohne Gewähr für Vollständigkeit oder Richtigkeit. Es wird keine Haftung übernommen für Schäden durch die Verwendung von Informationen aus diesem Online-Angebot oder durch das Fehlen von Informationen. Dies gilt auch für Inhalte Dritter, die über dieses Angebot zugänglich sind.

Radiolarian faunal turnover through the Paleocene-Eocene transition, Mead Stream, New Zealand

CHRISTOPHER J. HOLLIS¹

Key words: South Pacific, Paleogene, Radiolaria, diatoms, paleoecology, global change

ABSTRACT

The Mead Stream section, northern Clarence Valley, is the most complete Paleocene-early Eocene record of pelagic sedimentation in the mid-latitude (~55° S paleolatitude) Pacific Ocean. Integrated studies of sediments, siliceous and calcareous microfossils and carbon isotopes have shown that major global climate events are recorded by distinct changes in lithofacies and biofacies. The consistent and often abundant occurrence of siliceous microfossils in the section provides a rare opportunity to undertake quantitative analysis of high-latitude radiolarian population changes through the late Paleocene and early Eocene. Late Paleocene assemblages are dominated by spumellarians, although the nassellarian species *Buryella tetradica* is the most abundant species. The Paleocene-Eocene boundary (= base of Paleocene-Eocene thermal maximum) in the Mead Stream section is marked by major faunal turnover, including an abrupt decrease in *B. tetradica*, first occurrences of several low-latitude species (e.g. *Amphicraspedum prolixum* s.s., *Lychnocanium auxilla*, *Podocyrtis papalis*, *Phormocyrtis turgida*, *Theocorys? phyzella*) and increased abundance of large, robust spumellarians relative to small actinommids. Above an 18-m thick, lowermost Eocene interval in which radiolarians are abundant to common, radiolarian abundance declines progressively, falling to <10 individuals per gram in the marl-dominated unit that is correlated with the early Eocene climatic optimum. These trends in siliceous microfossil populations signal major changes in watermass characteristics along the northeastern New Zealand margin in the earliest Eocene. Assemblages typical of cool, eutrophic, watermasses that dominated the Marlborough Paleocene were replaced in the early Eocene by assemblages more characteristic of oligotrophic, stratified, subtropical-tropical watermasses.

ZUSAMMENFASSUNG

Das Mead Stream Profil, nördliches Clarence Tal, ist die vollständigste Paläozän-Früh Eozän Aufzeichnung pelagischer Sedimentation in mittleren Breiten (~55° S Paläobreite) des Pazifischen Ozeans. Integrierte Studien von Sedimenten, kieseligen und kalkigen Mikrofossilien und Kohlenstoffisotopen haben gezeigt, dass bedeutende globale Klimaereignisse durch deutliche Veränderungen in Litho- und Biofazies gekennzeichnet sind. Das beständige und oft sehr häufige Vorkommen kieseliger Mikrofossilien im Profil bietet eine seltene Gelegenheit, quantitative Studien von Veränderungen innerhalb von Radiolarienpopulationen hoher Breiten während des späten Paläozäns und frühen Eozäns durchzuführen. Spätpaläozäne Vergesellschaftungen werden von Spumellarien dominiert, obwohl die Nassellarienart *Buryella tetradica* die häufigste Art ist. Die Paläozän-Eozän Grenze (=Basis des Paläozän-Eozän Wärmemaximums) im Mead Stream Profil ist durch bedeutende faunistische Erneuerungen gekennzeichnet, einschließlich der abrupten Abnahme von *B. tetradica*, dem ersten Auftreten zahlreicher Arten niedriger Breiten (z. B. *Amphicraspedum prolixum* s.s., *Lychnocanium auxilla*, *Podocyrtis papalis*, *Phormocyrtis turgida*, *Theocorys? phyzella*) und der zunehmenden Häufigkeit von großen, robusten Spumellarien im Verhältnis zu kleinen Actinommida. Oberhalb eines 18 Meter mächtigen Intervalls des untersten Eozäns, in dem Radiolarien sehr zahlreich bis häufig sind, nimmt die Radiolarienhäufigkeit progressive ab, bis auf eine Anzahl von weniger als zehn Individuen pro Gramm innerhalb der Mergel-dominierten Einheit, die dem früheozänen Klimaoptimum entspricht. Diese Trends innerhalb von Populationen kieseliger Mikrofossilien signalisieren bedeutende Veränderungen in Wassermassencharakteristika entlang des nordöstlichen neuseeländischen Kontinentalrandes im frühesten Eozän. Vergesellschaftungen typisch für kühle, eutrophische Wassermassen, die das Marlborough Paläozän dominierten, wurden im frühen Eozän durch Vergesellschaftungen ersetzt, die eher für oligotrophische, stratifizierte, subtropische-tropische Wassermassen charakteristisch sind.

1. Introduction

Radiolaria are the most diverse and widely distributed group of marine plankton preserved in the fossil record (Lipps 1993; De Wever et al. 2001). High evolutionary turnover and considerable geographic variation in populations make radiolarian fossils invaluable research tools in biostratigraphy and paleoceanography. Consequently, detailed census studies through

sedimentary successions have the potential to reveal much about biosphere-geosphere interactions in the marine realm during critical episodes in Earth history. Whereas quantitative studies are common for late Cenozoic radiolarians (e.g. Boltovskoy 1987; Caulet et al. 1992), very few such studies have been made of early Cenozoic or Mesozoic assemblages.

¹ Institute of Geological and Nuclear Sciences, PO Box 30-368, Lower Hutt, New Zealand. Email: c.hollis@gns.cri.nz

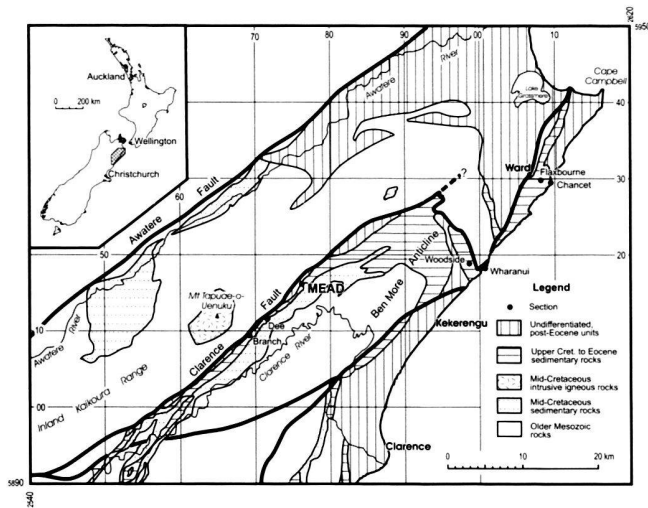


Fig. 1. Simplified geological map of eastern Marlborough (after Crampton et al. 2003) showing location of Mead Stream and other stratigraphic sections mentioned in the text.

Notable exceptions are studies of Cretaceous-Tertiary boundary radiolarians in New Zealand and Ecuador (Hollis 1996; Keller et al. 1997; Hollis et al. 2003a, b). In this article we report the results of the first quantitative study of radiolarian assemblage variation through the Paleocene-Eocene (P-E) transition (~60-50 Ma).

In addition, this is the first study of radiolarian faunal change through the P-E transition in the mid-latitude South Pacific; eastern Marlborough being situated at ~55° S in the latest Paleocene (King et al. 1999; Sutherland et al. 2001). Sanfilippo & Nigrini (1998a) reviewed DSDP and ODP records of late Paleocene-early Eocene radiolarians and established a composite biostratigraphy from well-preserved, low-latitude assemblages in 12 sites between 40°N and 30°S. Most of these sites are in the western central and North Atlantic, with two in the South Atlantic, one in the western central Indian Ocean and one in the North Pacific. Subsequently, Nigrini & Sanfilippo (2000) and Sanfilippo & Blome (2001) reported on radiolarian assemblages in well-constrained P-E boundary records in Caribbean and western North Atlantic ODP holes, respectively.

The section exposed in the southern branch of Mead Stream, Clarence River valley (Fig. 1), is the most complete known record of South Pacific pelagic-hemipelagic sedimentation from Late Cretaceous to middle Eocene (Strong et al. 1995; Hollis et al. 2005). Rich radiolarian assemblages make it a key reference section for early Paleogene radiolarian biostratigraphy and it is the type section for eight zones (RP6-13) in the South Pacific radiolarian zonation (Strong et al. 1995; Hollis 1997, 2002; Hollis et al. 2005). Detailed stratigraphic and paleoenvironmental studies have been completed on the Cretaceous/Tertiary (K/T) boundary (Hollis et al. 2003a) and the

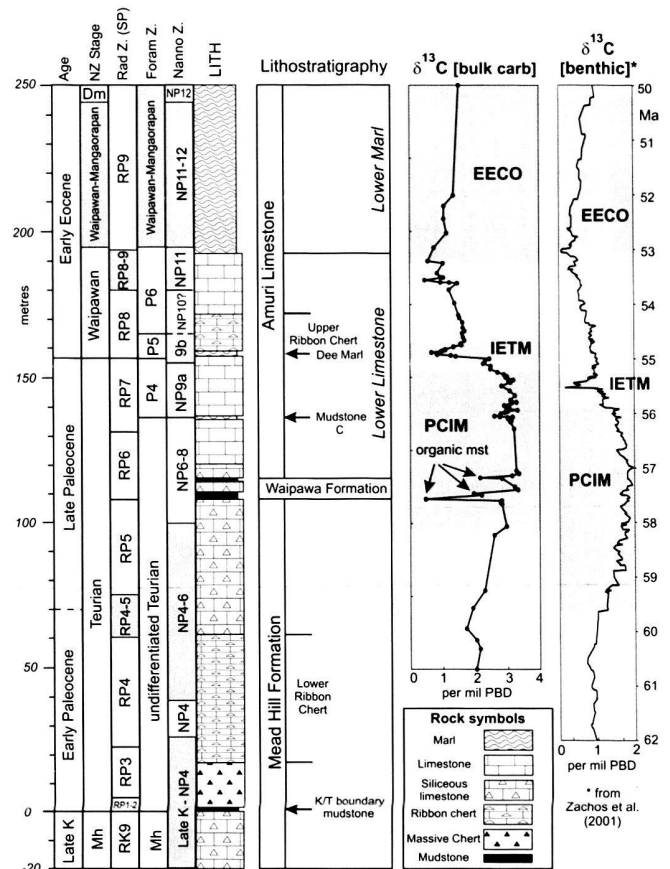


Fig. 2. Lithostratigraphy, biostratigraphy and carbon isotope stratigraphy of Upper Cretaceous-lower Eocene strata at Mead Stream (after Hollis et al. 2005). For age and biostratigraphy columns, intervals of uncertain age or biozone are shaded. Three episodes of major global change are identified from bulk carbonate $\delta^{13}\text{C}$ stratigraphy: late Paleocene carbon isotope maximum (PCIM), Paleocene-Eocene thermal maximum (PETM) and early Eocene climatic optimum (EECO). For comparison, the global compilation of benthic foraminiferal $\delta^{13}\text{C}$ data of Zachos et al. (2001) is also shown; the plotted values are running five-point averages calibrated to the geochronometric time scale of Berggren et al. (1995) following Hollis et al. (2005).

Paleocene-Eocene (P-E) transition (Hollis et al. 2005). In the latter study, carbon isotope stratigraphy was integrated with radiolarian, foraminiferal and calcareous nannofossil biostratigraphy in order to relate lithofacies changes to major perturbations in the early Paleogene global carbon cycle and climate system. Three of these episodes of perturbations have been identified in upper Paleocene and lower Eocene strata at Mead Stream (Fig. 2): the late Paleocene carbon isotope maximum (PCIM – Corfield & Cartlidge 1992, Thompson & Schmitz 1997; Kurtz et al. 2003), the Paleocene-Eocene thermal maximum (PETM – Zachos et al. 2001, 2003), and the early Eocene climatic optimum (EECO – Zachos et al. 2001). The base of the PETM corresponds with the Paleocene-Eocene boundary (Zachos et al. 2003). The aim of the current

study is to use changes in radiolarian assemblages through the P-E transition at Mead Stream to further elucidate the influence of these global events on oceanic conditions in the South-west Pacific.

2. Material and Methods

This study is based on 42 radiolarian assemblages recovered from rock samples between 100 and 250 m above the well-constrained K/T boundary (Hollis et al. 2003a) in the southern and main branch of Mead Stream. Sampling methods are described by Hollis et al. (2005). For radiolarian microfossil extraction, samples were crushed into 5–10 mm chips and leached in 15% hydrochloric acid (HCl) until reaction ceased. Siliceous rocks with weak reaction to HCl digestion were then rinsed and leached in 5% hydrofluoric acid for 2–4 hours. Samples were then washed through a 63 µm screen and the residues cleaned by gentle heating in a 1:1 solution of 10% hydrogen peroxide and calgon, (NaPO₃)₆.

Taxonomic nomenclature is summarised in Table 1. Selected species are illustrated in Plates 1–3. Census data (Hollis et al. 2005, supplementary data) have been derived from vertical traverses of strewn slides under transmitted light. For sparse samples (<300 radiolarians per slide), all radiolarians on one, two or more slides were counted. For richer samples, the following double count method was utilised. First, all specimens were counted until a total count of ~300 was achieved. The proportion of the slide examined to this point was determined and the abundance of common taxa (>15 radiolarians or >5% of the total fauna) was estimated for the remainder of the slide. The remainder of the slide was then examined and occurrences of rare taxa (<5% in initial count) recorded. This method has the advantage of establishing reliable abundance estimates for rare taxa without expending great amounts of time counting many hundreds of specimens. One disadvantage is that the total count is highly variable, ranging in this dataset from <60 to >7000 individuals. Abundance of larger (>63 µm) diatoms was also recorded during the initial count (Hollis et al. 2005).

In order to obtain an accurate estimate of relative abundance, all specimens have been assigned a taxonomic category. Although these counting groups range from the level of subspecies to family, they are given equal weighting in diversity analysis.

3. Stratigraphy

The lithostratigraphy and foraminiferal, radiolarian and dinoflagellate cysts biostratigraphy of Upper Cretaceous to middle Eocene strata at Mead Stream was described by Strong et al. (1995). Subsequently, the radiolarian biostratigraphy was reviewed and revised by Hollis (1997). Hollis et al. (2003a) described the stratigraphy of the K/T boundary transition in de-

tail, as part of a paleoenvironmental study of this interval at Mead Stream and nearby Branch Stream (Fig. 1). The K/T boundary is defined as zero datum in the current study. As a forerunner to the present study, Hollis et al. (2005) completed a detailed stratigraphic study of upper Paleocene-lower Eocene strata at Mead Stream, incorporating lithostratigraphy, foraminiferal, calcareous nannofossil and radiolarian biostratigraphy and carbon isotope stratigraphy (Fig. 2).

Paleocene-Eocene strata exposed along Mead Stream consist of well-bedded units of chert, siliceous limestone with chert nodules, siliceous mudstone, limestone and marl, which form three formations within the Muzzle Group (Reay 1993). The Mead Hill Formation consists of dm-bedded chert and siliceous limestone. It extends from a faulted base 170 m below the K/T boundary to a sharp contact with overlying the Waipawa Formation at 108 m above the K/T boundary. The Waipawa Formation is a 7.5 m thick interval (108–115.5 m) that consists of lower and upper siliceous mudstone units with an intervening unit of siliceous limestone. The two mudstone units carry the same distinctive geochemical signature of the Waipawa Formation as in its type area in Hawkes Bay, North Island (Killops et al. 2000).

The overlying formation, Amuri Limestone, has been subdivided into several lithotypes and members (Reay 1993; Hollis et al. 2005). The basal lithotype is Lower Limestone, which includes two members, Dee Marl and Upper Ribbon Chert. Lower Limestone (116–192 m) consists of dm-bedded siliceous limestone with thin marl interbeds and rare chert nodules. One unusually thick marl bed provides a useful reference point (136.5–136.6 m) within Lower Limestone and is referred to as Mudstone C (following Hollis et al. 2005). Dee Marl is a 2.4 m thick unit (157–159.4 m) of dm-bedded alternating marl and marly limestone. This unit marks the base of the Eocene at Mead Stream and at the type section, Dee Stream (Hancock et al. 2003). Upper Ribbon Chert, the highest occurrence of chert in the section, is a 12.6 m thick interval (159.4–172 m) of dm-bedded siliceous limestone with narrow chert stringers in the centre of the beds. The abundance of chert decreases gradually up-section, whereas the abundance and thickness of marl interbeds increases. The top of Lower Limestone is placed at the base of the first of a series of thick marl beds intercalated with limestone beds. The overlying lithotype, Lower Marl, consists of 110 m of alternating marl and marly limestone beds, similar to the lithology of Dee Marl. The stratigraphy of the upper part of Amuri Limestone, which is not considered here, is described by Strong et al. (1995).

4. Siliceous microfossil occurrence

Of 134 samples processed for radiolarians in upper Paleocene and lower Eocene strata at Mead Stream (~75–300 m), 42 samples contained radiolarian assemblages of adequate preservation and abundance for species level identification and quanti-

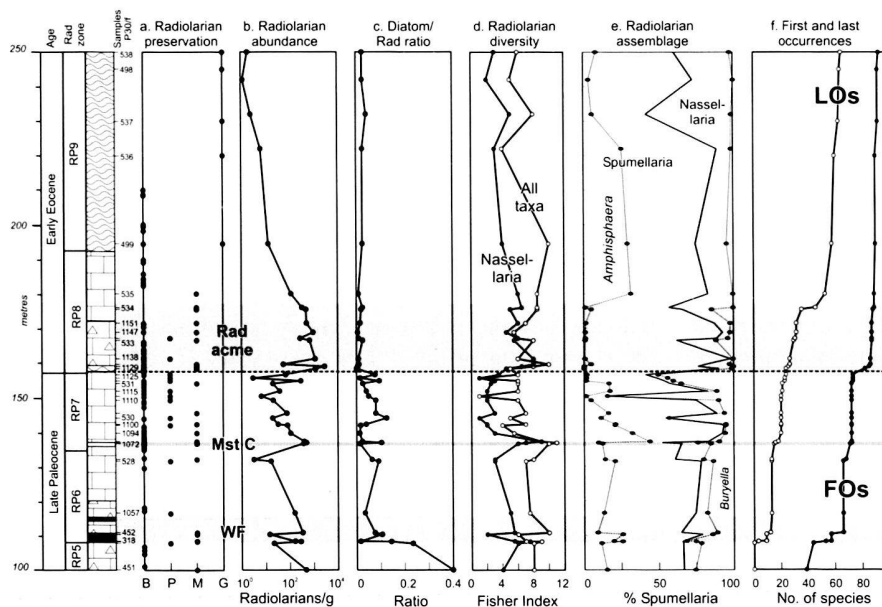


Fig. 3. Variation (a) radiolarian preservation, (b) radiolarian abundance, (c) diatom/radiolarian ratio, (d) radiolarian diversity (Fisher α Index), (e) relative abundance of major radiolarian groups, and (f) radiolarian first and last occurrences in upper Paleocene-lower Eocene siliceous microfossil assemblages at Mead Stream. Radiolarian preservation is recorded as Barren, Poor (internal and surface features obscured by recrystallisation), Moderate (internal features obscured by infilling or recrystallisation, surface features preserved), Good (test morphology not affected by recrystallisation, no infilling, breakage minor to moderate). Shaded intervals represent two distinctive units (WF = Waipawa Formation, Mst C = Mudstone C) and a 21 m-thick lowermost Eocene interval characterised by peak radiolarian abundances (rad acme).

tative analysis (Fig. 3). Radiolarians are generally common but poorly preserved in the upper Paleocene where strong recrystallisation, including siliceous infilling and overgrowth, is evident in siliceous limestone samples (Fig. 3a–b). In the first 21 m of Eocene strata, radiolarians are generally abundant and moderately preserved. Recrystallisation is less pronounced in this interval. This probably reflects reduced silica content in Dee Marl. In the overlying Upper Ribbon Chert, chertification is restricted to a central zone in each bed and samples taken from the outer parts of beds contained relatively well-preserved siliceous microfossils. In the overlying marl-rich Eocene interval, radiolarians are increasingly rare but preservation is moderate to good.

Diatoms are common in radiolarian residues in the Paleocene but are rare to very rare in the Eocene (Fig. 3c). The original change in diatom abundance across the P/E boundary is likely to have been even more pronounced than is described here. Owing to their smaller average size and more delicate tests, diatoms are more prone to diagenetic destruction than radiolarians. Therefore, diatoms are likely to be under-represented in Paleocene siliceous limestone samples relative to the better preserved Eocene material.

Radiolarian diversity is highly variable. Most assemblages contain 20–50 taxa whereas three assemblages have <20 taxa and seven assemblages have >50 taxa. The Fisher α Index is used to assess diversity trends in census data (Fig. 3d). The diversity curve for all taxa is considered to be less reliable than the curve for nassellarians. Most nassellarians have been identified to species level, whereas many spumellarians remain undifferentiated below family level. This results in an underestimate of overall diversity in spumellarian-dominated samples, notably in the earliest Eocene. Nassellarian α values indicate relatively low diversity in the Paleocene, apart from a short-

lived increase in the marl bed (Mudstone C) near the base of Zone RP7. A rapid increase in diversity in the earliest Eocene is followed by a gradual decline with relatively low α values through the Lower Marl.

Paleocene radiolarian assemblages are dominated by spumellarians (Fig. 3e) and, in order of abundance, the most common species and species groups are: *Buryella tetradica*, *Haliomma* spp. gr. b, *Amphisphaera coronata* gr. A. *goruna*, *Lithelius minor* gr. and *Buryella granulata*. In the lowermost 21 m of Eocene strata, spumellarian dominance is greater than in the Paleocene and the most common species are: *Haliomma* gr. b., *Amphisphaera coronata* gr. *Lithelius minor* gr. and *Theocorys?* cf. *physzella*. In overlying Eocene strata, spumellarians dominate to a similar extent as in the Paleocene and the most common species are: *Haliomma* gr. b, *Amphisphaera coronata* gr. *Lithelius minor* gr., *Calocycloma ampulla*, *Phormocyrtis striata striata*, *Podocyrtis papalis*, *Sethocyrtis babylo-nis*, *Axoprimum pierinae* and *Periphaena heliasteriscus*.

5. Radiolarian faunal turnover through the Paleocene-Eocene transition

In contrast to low-latitude regions where there is little change in radiolarian assemblages across the Paleocene-Eocene boundary (Sanfilippo & Nigrini 1998a; Nigrini & Sanfilippo 2000; Sanfilippo & Blome 2001), four episodes of significant faunal turnover are observed in the upper Paleocene-lower Eocene succession at Mead Stream (Fig. 3f, Table 2).

The first episode occurs in the lower Waipawa Formation and is associated with the RP5/RP6 zone boundary. The first occurrences (FOs) of 22 species and the last occurrences (LOs) of 12 species are recorded within 3 m of strata (~108–111 m). Some of the LOs are isolated records of Cretaceous-early Pa-

Table 1. Annotated list of radiolarian species or species groups encountered in this study. Species ranges are based on the South Pacific zonation for Mead Stream and other South Pacific ("Sth Pac") sections (Hollis, 1997, 2002; Hollis et al. 1997), and on the tropical zonation (Sanfilippo and Nigrini, 1998a) for low latitude ("Low Lat") records; LK = Late Cretaceous, UZP = unzoned Paleocene, EOC = Eocene, MIO = Miocene. Reference to taxon concept: CC42 = Clark and Campbell, 1942; F73 = Foreman, 1973; H02 = Hollis, 2002; H97a = Hollis, 1997; H97b = Hollis et al. 1997; K99 = Kozlova, 1999; N92 = Nishimura, 1992; S85 = Sanfilippo et al. 1985; SR92 = Sanfilippo and Riedel, 1992; S95 = Strong et al. 1995; SR73 = Sanfilippo & Riedel, 1973.

Taxon name	Zonal range			Taxon concept	
	Mead	Sth Pac	Low Lat.	Ref.	Strong et al. 1995:
<i>Amphicraspedum murrayanum</i> HAECKEL	RP8	RP8	RP6-8	SR73	
<i>Amphicraspedum prolixum</i> form. <i>gracilis</i> (LIPMAN)	RP8-9	RP8-9	?	K99	
<i>Amphicraspedum prolixum</i> SANFILIPPO & RIEDEL gr.	RP7-10	RP7-10	RP7-13	SR73	
<i>Amphicraspedum prolixum</i> SANFILIPPO & RIEDEL s.s.	RP8-10	RP8-10	RP7-9	RP7-9	208
<i>Amphipternis alamedaensis</i> (CAMPB. & CL.)	RP3-9	RK9-RP9	LK-RP7	H97a	
<i>Amphipyndax stocki</i> (CAMPB. & CLARK)	RK9-RP7	RK9-RP7	LK-UZP	H97a	
<i>Amphisphaera</i> aff. <i>magnaporulosa</i> CL. & CAMPB.	RP5-9	RP4-6	?	H02	
<i>Amphisphaera coronata</i> s.l. (EHRENBERG)	RP4-9	RP4-6	UZP-EOC	H97a	208 (<i>A. radiosa</i>)
<i>Amphisphaera goruna</i> (SANFILIPPO & RIEDEL)	RP3-8	RP2-6	UZP-RP7	H97a	208, fig. 8G, 9A
<i>Amphisphaera kina</i> HOLLIS	RP2-7	RP2-6	?	H97a	208, fig. 8F
<i>Amphisphaera macrosphaera</i> (NISHIMURA)	RP3-9	RP3-14	UZP-RP6	H97a	208 (<i>A. radiosa</i>)
<i>Amphymenium splendiaratum</i> CLARK & CAMPB.	RP6-8	RP2-6	RP8-20	H97a	
<i>Artostrobos pusillus</i> (EHRENBERG)	RK9-RP8	RK9-RP8	?	H97a	
<i>Aspis murus</i> NISHIMURA	RP6	RP5-6	RP6	N92	
<i>Axoprunum pierinae</i> (CLARK & CAMPB.)	RP5-9	RP6-14	UZP-EOC	SR73	208, fig. 10C
<i>Axoprunum</i> ? aff. <i>bispiculum</i> (POPOFSKY)	RP6-9	RP4-6	?	H02	
<i>Bathropyramis magnifica</i> (CLARK & CAMPB.)	RP5-13	RP4-13	?	H02	
<i>Bathropyramis sanjoaquinensis</i> (CAMPB. & CLARK)	RK9-RP8	RK9-RP8	LK-UZP	H97a	
<i>Bekoma bidartensis</i> RIEDEL & SANFILIPPO	RP8	RP8	RP7-8	S95	208, fig. 9G
<i>Bekoma campechensis</i> FOREMAN	RP6	RP6	RP6-7	S95	208, fig. 9F
<i>Bekoma divaricata</i> FOREMAN	RP6-8	RP6-8	RP7	S95	208, fig. 9H
<i>Buryella dumitricai</i> PETRUSHEVSKAYA	RP4-7	RP4-7	?	H97a	208, fig. 8L-M
<i>Buryella foremanae</i> PETRUSHEVSKAYA	RP4-7	RP4-7	?	H97a	208, fig. 8K
<i>Buryella granulata</i> (PETRUSHEVSKAYA)	RP3-8	RP4-8	?	H97a	208, fig. 8J
<i>Buryella helenae</i> O'CONNOR	RP6	RP4-6	?	H02	
<i>Buryella kaikoura</i> HOLLIS	RP5-6	RP5-6	?	H97a	
<i>Buryella pentadica</i> FOREMAN	RP6	RP6	UZP-RP7	N92	
<i>Buryella petrushevskayae</i> O'CONNOR	RP6	RP5-6	?	H02	
<i>Buryella tetradica tetradica</i> FOREMAN	RP5-9	RP5-8	UZP-RP9	H02	208, fig. 8N, 9Q-R
<i>Buryella tetradica tridica</i> O'CONNOR	RP6	RP5-6	?	H02	
<i>Calocycloma ampulla</i> (EHRENBERG)	RP5-10	RP5-10	RP6-14	S95	208, fig. 9V-X
<i>Cassideus</i> aff. <i>mariae</i> NISHIMURA	RP5-9	RP5-9	?	H02	209, fig. 9C (<i>Microsciadiocapsa</i> ? sp.)
<i>Clathrocyclas australis</i> HOLLIS	RP3-6	RP2-6	?	H97a	P. 208, 8P (<i>Clathrocycloma</i> sp. A)
<i>Clathrocyclas universa</i> gr.	RP5-13	RP5-13	?	H97b	
<i>Conoactinomma stiliformis</i> (LIPMAN)	RP9	RP9	?	K99	206 (<i>Conocaryomma</i> sp.)
<i>Cornutella californica</i> CAMPB. & CLARK	RK9-RP13	RK9-RP13	LK-UZP	H97a	
<i>Corythomelissa adunca</i> (SANFILIPPO & RIEDEL)	RP5-8	RP4-8	RP6-8	H02	208, fig. 9B
<i>Corythomelissa</i> spp.	RP6-8	RP6-8	?	H02	
<i>Cryptocarpium</i> ? cf. <i>ornatum</i> (EHRENBERG)	RP6-13	RK9-RP13	?	H97a	
<i>Cycladophora</i> aff. <i>cosma</i> LOMBARI AND & LAZARUS	RP6-8	RP4-8	?	H02	
<i>Cycladophora</i> cf. <i>bicornis</i> (POPOFSKY)	RP6-8	RP6-8	?	H02	208, fig. 9D (<i>Clathrocycl. humerus</i>)
<i>Dictyomitra andersoni</i> (CAMPB. & CLARK)	RK9-RP6	RK9-RP6	LK-UZP	H97a	
<i>Haliomma</i> gr. B	RP4-9		H97a		
<i>Lamptonium fabaeforme fabaeforme</i> (KRASHEN.)	RP8-9	RP8-9	RP7-9	S85	
<i>Lamptonium pennatum</i> FOREMAN	RP7-9	RP7-9	UZP-RP8	S95	208, fig. 9I
<i>Lamptonium</i> ? aff. <i>colymbus</i> FOREMAN	RP9		F73		
<i>Lithelius</i> ? <i>minor</i> gr. JØRGENSEN	RK9-RP9	RK9-RP14	?	H97a	
<i>Lithocampe wharanui</i> HOLLIS	RP3-6	RK9-RP6	?	H97a	
<i>Lithomespilus coronatus</i> SQUINABOL	RK9RP7	RK9-RP8	UZP-RP8	H97a	
<i>Lithostrobos longus</i> GRIGORJEVA	RP1-7	RP1-6	?	H02	209, fig. 8H-I (<i>Stichomitra wero</i>)
<i>Lophophaena mugaica</i> (GRIGORJEVA)	RP5-8	RP2-8	?	H02	

Table 1. (cont.)

Taxon name	Zonal range			Taxon concept	
	Mead	Sth Pac	Low Lat.	Ref.	Strong et al. 1995:
<i>Lychnocanium</i> aff. <i>carinatum</i> EHRENBERG	RP8	RP8	RP6-7	N92	209, fig. 9M (<i>Rhopalocanium?</i> sp.)
<i>Lychnocanium</i> aff. <i>tripodium</i> EHRENBERG	RP7-8	RP7-8	?	K99	
<i>Lychnocanium</i> <i>amphitrite</i> (FOREMAN)	RP9-13	RP9-14	RP8-20	F73	
<i>Lychnocanium</i> <i>auxilla</i> (FOREMAN)	RP8	RP8	RP6-7	F73	
<i>Lychnocanium</i> <i>bellum</i> CLARK & CAMPB.	RP9-13	RP9-14	RP8-14	F73	209, fig. 11I-J (as <i>Lychnocanoma</i>)
<i>Lychnocanium</i> <i>satelles</i> (KOZLOVA)	RP5-9	RP5-9	?	H02	208, fig. 9L (<i>L. auxilla</i>)
<i>Lychnocanium</i> sp. B	RP7-8		?	S95	209, fig. 9J
<i>Lychnocanium</i> <i>zhamoidai</i> KOZLOVA	RP7-9		?	K99	209, fig. 9K (<i>Lychnocanoma</i> sp. A)
<i>Middourium</i> <i>regulare</i>	RP6-8	RP6-8	RP6-7	K99	
<i>Mita</i> <i>regina</i> (CAMPB. & CLARK)	RK9-RP6	RK9-RP6	LK-UZP	H97a	
<i>Mita</i> sp. A (? = <i>Siphocampe?</i> "eilizabethae")	RP9-10	RP9-RP15	?	S95	209, fig. 10X
<i>Monobrachium</i> <i>irregulare</i>	RP7-8	RP7-8	RP6-7	K99	
<i>Myllocercion</i> <i>acineton</i> FOREMAN	RK9-RP6	RK9-RP4	LK-UZP	H97a	
<i>Orbiculiforma</i> <i>renillaeformis</i> gr. (CAMPB. & CL.)	RK9-RP6	RK9-RP6	LK-UZP	H02	
<i>Patagospyrus</i> <i>confluens</i> (EHRENBERG)	RP4-RP8	RP4-8	UZP-RP10	K99	
<i>Periphaena</i> <i>alveolata</i> (LIPMAN)	RP5-9	RP5-9	?	K99	
<i>Periphaena</i> <i>heliasteriscus</i> (CLARK & CAMPB.)	RP8-9	RP6-9	UZP-EOC	SR73	
<i>Peritiviator?</i> <i>dumitricai</i> NISHIMURA	RP5-7	RP5-6	UZP-RP6	N92	
<i>Petalospyris</i> <i>foveolata</i> EHRENBERG	RP5-9	RP5-9	?	K99	209, fig. 8Q-R
<i>Petalospyris</i> <i>senta</i> (KOZLOVA)	RP6-9	RP6-9	?	K99	209, fig. 8S
<i>Phacostaurus?</i> <i>quadratus</i> NISHIMURA	RP6-7	RP6	RP6-7	N92	
<i>Phormocyrtis</i> <i>cubensis</i> (RIEDEL & SANFILIPPO)	RP8	RP8	RP6-8	F73	
<i>Phormocyrtis</i> <i>striata exquisita</i> (KOZLOVA)	RP7-8	RP7-8	RP6-9	S95	209, fig. 9N
<i>Phormocyrtis</i> <i>striata striata</i> (BRANDT)	RP7-10	RP7-10	RP7-14	S95	209, fig. 9O-P
<i>Phormocyrtis</i> <i>turgida</i> (KRASHENINNIKOV)	RP8	RP8	RP6-8	F73	
<i>Plectodiscus</i> <i>circularis</i> (CLARK & CAMPB.)	RP6-8	RP6-8	RP6-EOC	PK72	
<i>Podocyrtis</i> <i>acalles</i> SANFILIPPO & RIEDEL	RP8-9	RP8-9	RP8-9	S92	209, fig. 9T-U (<i>P. aphorma</i>)
<i>Podocyrtis</i> <i>papalis</i> EHRENBERG	RP8-10	RP8-14	RP7-18	S92	209, fig. 9S
<i>Pterocodon</i> <i>poculum</i> NISHIMURA	RP6-7	RP6-7	RP6-7	H02	
<i>Saturnalis</i> <i>kennetti</i> DUMITRICA	RP3-8	RP1-8	?	H97a	
<i>Sethochytris</i> <i>babylonis</i> (CLARK & CAMPB.) gr.	RP6-13	RP6-15	RP6-20	H02	208, fig. 11A-B (as <i>Lychnocanoma</i>)
<i>Siphocampe</i> <i>nodosaria</i> (HAECKEL)	RP6-13	RP4-15	RP6-14	H02	209 (<i>S. arachnaea</i>)
<i>Siphocampe</i> <i>quadrata</i> (PETRUSHEV. & KOZLOVA)	RP8-13	RP5-15	RP6-20	H02	209, fig. 10R
<i>Spongurus</i> <i>bilobatus</i> gr. CLARK & CAMPB.	RP5-9	RP4-9	?	H02	
<i>Stichomitra</i> <i>carnegiense</i> CAMPB. & CLARK	RK9-RP6	RK9-RP6	LK-UZP	H97a	
<i>Stylodictya</i> <i>targaeformis</i> CLARK & CAMPB.	RP5-9	RP5-9	?	CC42	
<i>Stylosphaera</i> <i>minor</i> CLARK & CAMPB.	RP3-9	RP3-6	UZP-MIO	H97a	
<i>Theocampe</i> <i>urceolus</i> (CAMPB. & CLARK)	RP9-13	RP9-15	RP8-20	S95	209, fig. 10Q
<i>Theocampe</i> <i>vanderhoofi</i> (CAMPB. & CLARK)	RK9-RP6	RK9-RP6	LK-UZP	H97a	
<i>Theocorys?</i> aff. <i>phyzella</i> FOREMAN	RP6-8	RP6-8	?	H02	208, fig. 9E (<i>Calocyclus asperum</i>)
<i>Theocorys?</i> cf. <i>phyzella</i> FOREMAN	RP7-8	?	RP7	SB01	(as <i>Theocorys</i> aff. <i>phyzella</i>)
<i>Theocorys?</i> <i>phyzella</i> FOREMAN	RP8		RP7-8	F73	
<i>Tholodiscus</i> <i>densus</i> (KOZLOVA)	RP6-8	RK9-RP8	?	H97a	

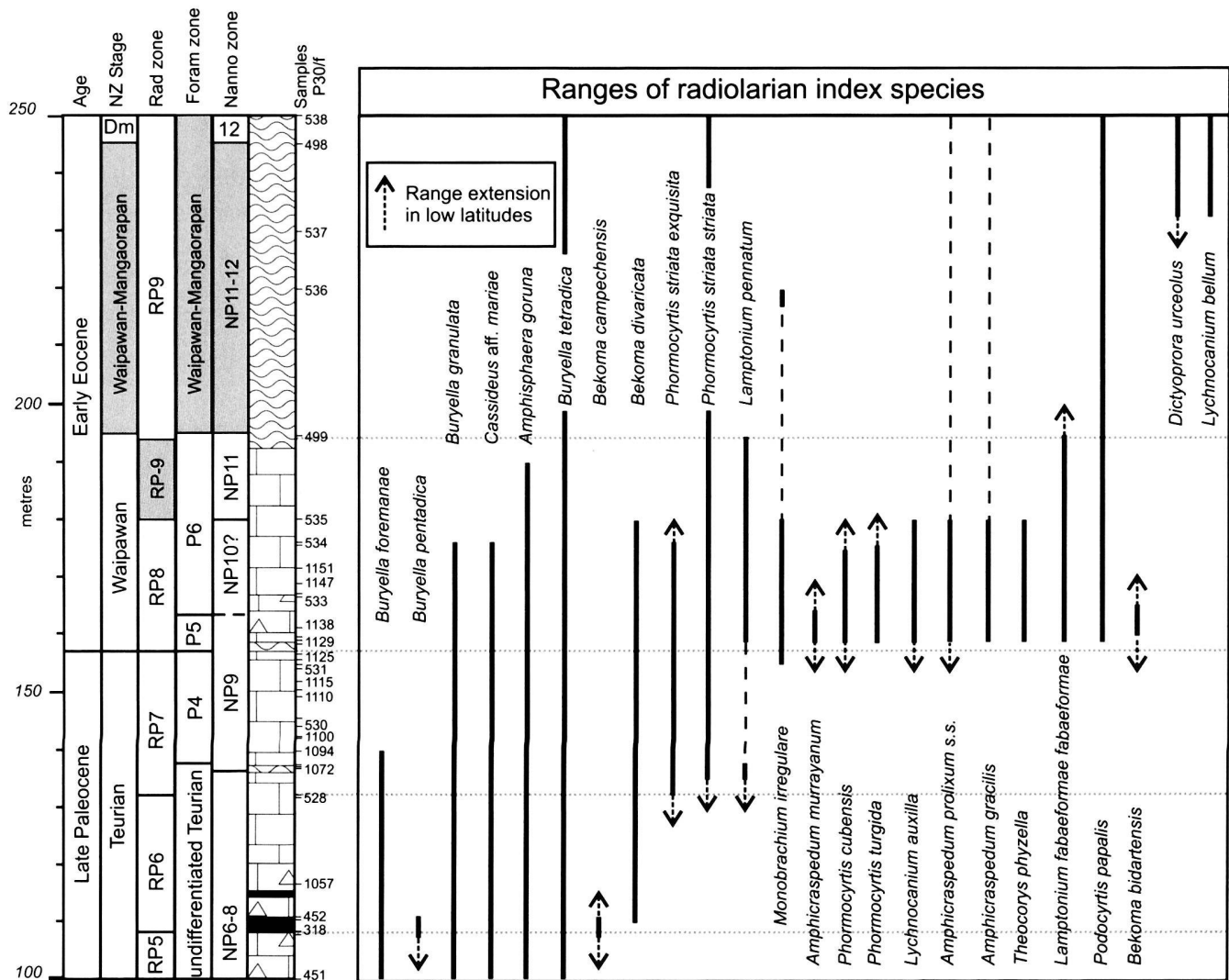


Fig. 4. Ranges of radiolarian index species in upper Paleocene-lower Eocene strata at Mead Stream. For age and biostratigraphy columns, intervals of uncertain age or biozone are shaded. Low-latitude ranges are based on (Sanfilippo & Nigrini 1998a, b) and Sanfilippo & Blome (2001).

leocene species (e.g. *Lithocampe wharanui*, *Mita regina*, *Myllocercion acineton*) that may be reworked into the siliciclastic Waipawa Formation. Other events are isolated records of taxa that are largely restricted to two particularly rich and diverse assemblages (P30/f318, f452), e.g. *Buryella helenae*, *B. petrushevskayae*, *Cryptocarpium* cf. *ornatum*. As most of the FOs recorded in this interval relate to species that are known to have earlier local FOs (Hollis 1997, 2002), this episode is not thought to reflect a time of high evolutionary turnover. Instead, the large number of events at the base of the Waipawa Formation suggests that either the unit is highly condensed or that there is a basal unconformity.

The second episode occurs within or directly below the 10 cm thick marl bed (Mudstone C). The FOs of 6 species and the LOs of 5 species occur within 5 m of strata. Most of the

LOs are the last record of Cretaceous-Paleocene species that are generally very rare in the upper Paleocene but are present in one or more of three relatively rich samples in this interval (P20/f1072, f1076, f1081); two of these species may be reworked into Mudstone C (*Amphipyndax stocki*, *Theocampe vanderhoofi*). Three species with FOs in this interval are key index species that have much earlier FOs in low latitudes (*Lamptonium pennatum*, *Phormocyrtis striata exquisita*, *P. s. striata* – Fig. 4). All are very rare in overlying Paleocene strata but occur consistently in the lowermost Eocene.

The third faunal turnover episode occurs at the base of the Dee Marl (Fig. 3f, Table 2). The FOs of 13 species are recorded within the first 3 m of Eocene strata at Mead Stream, with 9 of these species in the basal Eocene sample. Four of these species appear to be global markers for the P/E boundary

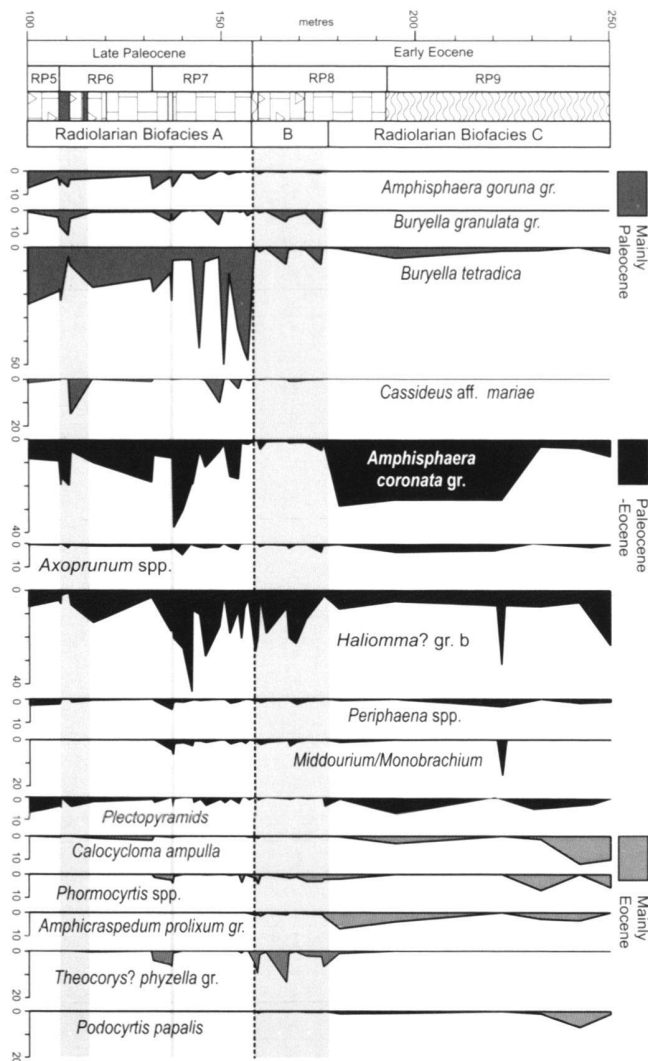


Fig. 5. Relative abundance of common radiolarian species and species groups in upper Paleocene-lower Eocene strata at Mead Stream.

(Sanfilippo & Nigrini 1998a; Sanfilippo & Blome 2001): *Lamp-tonium fabaeforme fabaeforme*, *Podocytis papalis*, *Phormocytis turgida* and *Theocorys? physzella* (Fig. 4). Five of the species are index species with late Paleocene FOs in low latitudes (Sanfilippo & Nigrini 1998a, b): *Amphicraspedum murrayanum*, *A. prolixum* s.s., *Bekoma bidartensis*, *Lychnocanium auxilla*, *Phormocytis cubensis* (Fig. 4).

There are relatively few significant LOs associated with the P/E boundary (Fig. 3f). The LOs of *Lithomespilus coronatus*, *Lithostrobos longus* and *Theocorys? aff. physzella* occur within the uppermost 3 m of Paleocene strata. Of the three LOs that occur within the basal Eocene Dee Marl, two are species that are restricted to the unit (*Amphicraspedum murrayanum*, *Lychnocanium* aff. *tripodium*) while one is the LO of a sporadically occurring late Paleocene species (*Cycladophora* aff. *cosma*). In contrast to the faunal changes observed at the base

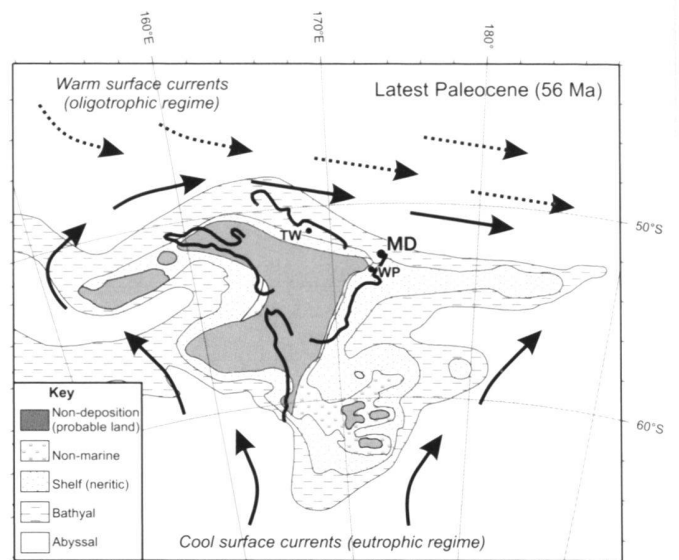


Fig. 6. Paleogeographic reconstruction of New Zealand region during the latest Paleocene (adapted from King et al. 1999) showing major current systems based on coupled climate model simulations for the Eocene (Huber 2002)

of the Waipawa Formation, the low number of LOs relative to FOs in the P/E boundary interval indicates that the faunal turnover is not due to a stratigraphic discontinuity. The abrupt appearance of many low-latitude species indicates that warming at the PETM promoted pole-ward migration of warm-water radiolarians. Similar, but less extreme, short-lived warming may explain the FOs of several low-latitude species around the time of deposition of Mudstone C (Fig. 3f, Table 2).

The final episode of marked faunal change in the studied section occurs ~20 m above the P/E boundary (Fig. 3f, Table 2). Within the same 5 m interval in which radiolarian abundance begins to decrease (175–180 m), the LOs of 21 species are recorded. These species include many that thrived through much of the late Paleocene as well as many that appeared in the earliest Eocene (Fig. 4). Only two FOs are recorded in this interval, one of these being the FO of the common Eocene phacodiscid *Periphaena heliasteriscus*. The high number of LOs, coupled with the onset of long term decline in radiolarian abundance and diversity, indicates that this episode of faunal change reflects a oceanographic changes unfavourable to all radiolarians.

6. Radiolarian biofacies

To simplify the discussion and presentation of census data (Fig. 5) in this section, some species are combined into larger groups that reflect a close phylogenetic relationship or morphological similarity:

1. *Amphisphaera coronata* gr. (*A. macrosphaera*, *A. coronata* s.l, *A. aff. magnaporulosa*).

2. *Amphisphaera goruna* gr. (*A. kina*, *A. goruna*)
3. *Axoprimum* spp. (*Axoprimum pierinae*, *A. aff. bispiculum*)
4. *Buryella granulata* gr. (*B. granulata*, *B. foremanae*, *B. dumitricai*)
5. *Middourium/Monobrachium* (*Middourium regulare*, *Monobrachium irregulare*)
6. *Periphaena* spp. (*Periphaena alveolata*, *P. heliasteriscus*)
7. *Phormocyrtis* spp. (*Phormocyrtis cubensis*, *P. striata exquisita*, *P. striata striata*, *P. turgida*)
8. Plectopyramidins (*Bathropyramis* and *Cornutella* spp.)
9. *Theocorys? phyzella* gr. (*Theocorys? cf. phyzella*, *Theocorys? phyzella*)

Three radiolarian biofacies are identified in the Paleocene-Eocene section at Mead Stream: (A) upper Paleocene (100–157 m), (B) lowermost Eocene (157–178 m) and (C) lower Eocene (178–250 m).

Biofacies A is characterised by abundant *Buryella tetradica*, common to abundant *Amphisphaera coronata* gr. and *Haliomma* gr. b, and few to common *Amphisphaera goruna* gr., *Buryella granulata* gr. and *Cassideus aff. mariae* (Fig. 5). Diatoms are common in this biofacies (Fig. 3c) and sediments are moderately siliceous, with a highly siliceous facies of the organic-rich Waipawa Formation (Killops et al. 2000) occurring in the lower part of the interval. Faunal similarities with diatom-rich, biosiliceous Paleocene lithofacies lower in the Marlborough sequence (Hollis et al. 1995, 2003a, b) and on the eastern margin of Campbell Plateau (Hollis 2002) suggest moderately eutrophic conditions, consistent with weak to moderate upwelling in outer shelf to upper slope depths (Fig. 6).

This biofacies spans an interval correlated with the PCIM, which is interpreted as a 3 m.y. episode of enhanced global carbon burial, either through increased marine or terrestrial productivity (Corfield & Cartlidge 1992; Thompson & Schmitz 1997; Kurtz et al. 2003). The regional occurrence of organic-rich mudstone in the lower part of the interval (Killops et al. 2000; Hollis et al. 2005) and abundant siliceous microfossils (Hollis 2002) indicates that this event is associated with enhanced marine productivity in the New Zealand region.

Biofacies B occurs in the lowermost 21 m of Eocene strata (157–178 m). It is characterised by abundant *Haliomma* gr. b and few to common *Phormocyrtis* spp. and *Theocorys? phyzella* gr. (Fig. 5). The base of the biofacies coincides with the P/E boundary and the onset of the PETM. A marked increase in radiolarian abundance and diversity is associated with a sharp decline in diatom abundance and in the abundance of *Buryella tetradica* – the dominant radiolarian species in the upper Paleocene (Fig. 3b–d, f). This species and *B. granulata* s.s. are rare in this interval, apart from two samples in which both species are common (P30/f533, f1223). The high abundance of large, robust spumellarians, namely *Haliomma* gr. b, *Middourium/Monobrachium* gr. and *Periphaena alveolata*, is a distinctive feature of Biofacies B. These taxa tend to be most abundant in marl samples of Dee Marl and are also common to abundant in underlying Paleocene marly layers, notably at

~137 and ~142 m, and overlying Eocene marl layers (Fig. 5). Despite the significant lithologic change from Dee Marl to Upper Ribbon Chert, there is little change in siliceous microfossil assemblages. A slight increase in biosiliceous productivity in Upper Ribbon Chert may be inferred from the increase in silica content and a small increase in diatom abundance, although overall radiolarian abundance and diversity declines (Fig. 3b–d).

Biofacies B has unusual characteristics that make interpretation difficult. The presence of many low-latitude species indicates relatively warm climatic conditions. The low abundance of diatoms and of radiolarian taxa characteristic of the eutrophic Paleocene Biofacies A, suggests conditions of relatively low productivity. However, radiolarian abundance and diversity maxima are recorded in Dee Marl and in underlying Mudstone C, which also contains an assemblage similar to Biofacies B. A very similar assemblage is present in lowermost Eocene carbonate ooze at high-latitude DSDP Site 277, southwest Campbell Plateau (Hollis et al. 1997). The three features of high total abundance, high diversity and high numbers of warm-water species are consistent with late Cenozoic tropical radiolarian assemblages (Casey 1993). This suggests that the PETM may have promoted the expansion of weakly eutrophic subtropical water into the Southwest Pacific (Fig. 6). Further biogeographic study of the distinctive spumellarians that dominate this biofacies is required to confirm this interpretation.

Biofacies C occurs in the upper part of the lower Eocene sequence (178 to 250 m). It is characterised by abundant *Amphisphaera coronata* gr., *Haliomma* gr. b, common *Calocyclus ampulla*, few to common *Phormocyrtis striata striata* and few to rare *Amphicraspedum prolixum* gr., *Axoprimum* spp., *Buryella tetradica*, *Periphaena heliasteriscus*, plectopyramidins, *Podocyrtis papalis* and *Sethochytris babylonis* gr. An upwards decrease in radiolarian abundance and diversity, coupled with low diatom abundance, indicates that this biofacies represents relatively oligotrophic conditions. Similar assemblages are found in lower Eocene carbonate ooze at DSDP site 277 (Hollis et al. 1997). As this biofacies is correlated with the EECO, it seems likely that global warming associated with this event promoted the expansion of oligotrophic subtropical water-masses into the Southwest Pacific.

7. Conclusions

The first quantitative study of radiolarian assemblages from an upper Paleocene-lower Eocene bathyal succession has identified three distinct biofacies that can be used to determine the influence of major changes in the global carbon cycle and climate system on Southwest Pacific oceanic conditions.

Biofacies A is associated with the PCIM, a 3 m.y. episode of maximum $\delta^{13}\text{C}$ values that is inferred to represent high rates of carbon burial due to enhanced marine or terrestrial productivity (Corfield & Cartlidge 1992; Thompson & Schmitz 1997; Kurtz et al. 2003). Hollis et al. (2005) argued that Mead Stream lithofacies, including organic mudstone and siliceous limestone,

are indicative of enhanced marine productivity in the Marlborough basin during the PCIM. Siliceous microfossil assemblages also indicate enhanced marine productivity. Biofacies A is associated with common diatoms and is dominated by the same or similar species that are found in biogenic silica-rich lithologies in the lower Paleocene in Marlborough (Hollis et al. 2003a, b) and in the upper Paleocene of the Campbell Plateau margin (Hollis 2002). Deposition of radiolarian and diatom-rich sediments in the Marlborough basin, as well as on the northwest and southeast continental margin of New Zealand, in the late Paleocene between ~60–56 Ma indicates that the PCIM was associated with enhanced marine productivity, at least in the southern Pacific Ocean. This is consistent with ocean circulation models for the South Pacific (Huber 2002).

Biofacies B is associated with the PETM, a 100–200,000 yr episode of extreme global warmth recorded as pronounced negative $\delta^{13}\text{C}$ and $\delta^{18}\text{O}$ excursions (Zachos et al. 2001), which at Mead Stream is associated with a lithofacies change from siliceous limestone to marly limestone and marl (Dee Marl). A marl bed (Mudstone C) ~20 m below the PETM may represent a precursor event. Not only is the bed also associated with a negative $\delta^{13}\text{C}$ excursion, but radiolarian assemblages are very similar to those of Biofacies B. Biofacies B is characterised by high radiolarian abundance and diversity, but very low diatom abundance. It is dominated by large, robust smooth-walled spumellarians of uncertain biogeographic affinity, and contains the only local record of several low-latitude species. The biofacies records an abrupt warm-water incursion in the East Coast Basin. The combination of an incursion of subtropical water and waning cool-water upwelling may have promoted an unusual bloom of warm water species. The occurrence of similar earliest Eocene radiolarian assemblages at New Zealand's southern continental margin (Hollis et al. 1997) indicates that warm subtropical waters may have extended as far south as 60°.

Biofacies C is associated with the onset of the EECO, a 3 m.y. episode of extreme global warming (Zachos et al. 2001), which at Mead Stream is associated with the transition from limestone- to marl-dominated sedimentation. Biofacies C is characterised by declining radiolarian abundance and diversity and low diatom abundance, implying a marked decrease in biosiliceous productivity. Significantly, many low-latitude as well as high-latitude radiolarian species disappear at the onset of the EECO. With similar early Eocene radiolarian assemblages recorded from the southern Campbell Plateau (Hollis et al. 1997), progressive warming is inferred to have promoted increasingly oligotrophic oceanic conditions around New Zealand.

Acknowledgements

Sample collection and stratigraphic integration was carried out with the assistance of Jerry Dickens, Brad Field, Craig Jones and Percy Strong. Samples were processed and slides were prepared by Kellee Anderson, Neville Orr and John Simes. The manuscript benefited for careful reviews by Annika Sanfilippo, Akiko Nishimura, James Crampton, Erica Crouch and Percy Strong. This research was supported by the Foundation for Research Science and Technology (GNS Global Change Through Time Programme, Contract CO5X0202).

REFERENCES

- BERGGREN W., KENT D., SWISHER C. & AUBRY M.-P. 1995: A revised Cenozoic geochronology and chronostratigraphy. In: BERGGREN, W. et al. (Eds): Geochronology, time scales and global stratigraphic correlation, 129–212, SEPM Special Publication 54.
- BOLTOVSKY D. 1987: Sedimentary record of radiolarian biogeography in the equatorial to Antarctic western Pacific Ocean. *Micropaleontology* 33, 267–281.
- CASEY R. 1993: Radiolaria. In: LIPPS, J.H. (Ed.): Fossil Prokaryotes and Protists, 249–284. Blackwell Scientific Publications, Oxford/London, UK.
- CAULET J., VENEC-PEYRE M.-T., VERGNAUD-GRAZZINI C. & NIGRINI C. 1992: Variation of South Somalian upwelling during the last 160 ka: radiolarian and foraminifera records in core MD 85674. In: SUMMERHAYES, C. et al. (Eds): Upwelling Systems: Evolution since the Early Miocene, Geological Society of London, Special Publication 64, 379–389.
- CORFIELD R. M. & CARLIDGE J. E. 1992: Oceanographic and climatic implications of the Palaeocene carbon isotope maximum. *Terra Nova* 4, 443–455.
- CRAMPTON J., LAIRD M., NICOL A., TOWNSEND D. & VAN DISSEN R. 2003: Palinspastic reconstructions of southeastern Marlborough, New Zealand, for Late Cretaceous to Eocene times. *New Zealand Journal of Geology and Geophysics* 46, 153–175.
- DE WEVER P., DUMITRICA P., CAULET J.-P., NIGRINI C. & CARIDROIT M. 2001: Radiolarians in the sedimentary record. 533 p., Gordon and Breach Science Publishers, The Netherlands.
- HANCOCK H., DICKENS G., STRONG C., HOLLIS C. & FIELD B. 2003: Foraminiferal and carbon isotope stratigraphy through the Paleocene-Eocene transition at Dee Stream, Marlborough, New Zealand. *New Zealand Journal of Geology and Geophysics* 46, 1–19.
- HOLLIS C. 1996: Radiolarian faunal change through the Cretaceous-Tertiary transition of eastern Marlborough, New Zealand. In: MACLEOD, N. & KELLER, G. (Eds): Cretaceous-Tertiary Mass Extinctions: Biotic and Environmental Changes, 173–204, Norton Press, New York.
- 1997: Cretaceous-Paleocene Radiolaria from eastern Marlborough, New Zealand. Institute of Geological and Nuclear-Sciences Monograph 17, 152 p.
- 2002: Biostratigraphy and paleoceanographic significance of Paleocene radiolarians from offshore eastern New Zealand. *Marine Micropaleontology* 46, 265–316.
- HOLLIS C., DICKENS G., FIELD B., JONES C. & STRONG C. 2005: The Paleocene-Eocene transition at Mead Stream, New Zealand: a southern Pacific record of early Cenozoic global change. *Palaeogeography, Palaeoclimatology, Paleoecology* 215, 313–343.
- HOLLIS C., RODGERS K. & PARKER R. 1995: Siliceous plankton bloom in the earliest Tertiary of Marlborough, New Zealand. *Geology (Boulder)* 23, 835–838.
- HOLLIS C., WAGHORN D., STRONG C. & CROUCH E. 1997: Integrated Paleogene biostratigraphy of DSDP site 277 (Leg 29): foraminifera, calcareous nannofossils, Radiolaria, and palynomorphs. Institute of Geological & Nuclear Sciences Science Report 97/7, 1–73.
- HOLLIS C., RODGERS K., STRONG C., FIELD B. & ROGERS K. 2003a: Paleoenvironmental changes across the Cretaceous/Tertiary boundary in the northern Clarence Valley, southeastern Marlborough, New Zealand. *New Zealand Journal of Geology and Geophysics* 46, 209–234.
- HOLLIS C., STRONG C., RODGERS K. & ROGERS K. 2003b: Paleoenvironmental changes across the Cretaceous/Tertiary boundary at Flaxbourne River and Woodside Creek, eastern Marlborough, New Zealand. *New Zealand Journal of Geology and Geophysics* 46, 177–197.
- HOLLIS C., DICKENS G., FIELD B., JONES C. & STRONG C. 2005: The Paleocene-Eocene transition at Mead Stream, New Zealand: a southern Pacific record of early Cenozoic global change. *Palaeogeography, Palaeoclimatology, Paleoecology* 215, 313–343.
- HUBER M. 2002: Straw man 1; preliminary view of the tropical Pacific from a global coupled climate model simulation of the early Paleogene. Proceedings of the Ocean Drilling Program, initial reports, Paleogene equatorial transect, Leg 199. Proceedings of the Ocean Drilling Program, Part A: Initial Reports 199, 30.

- KELLER G., ADATTE T., HOLLIS C., ORDONEZ M., ZAMBRANO I., JIMENEZ N., STINNESBECK E., ALEMAN A. & HALE-ERLICH W. 1997: The Cretaceous/Tertiary boundary event in Ecuador: reduced biotic effects due to eastern boundary current setting. *Marine Micropaleontology* 31, 97–133.
- KILLOPS S., HOLLIS C., MORGANS H., SUTHERLAND R., FIELD B. & LECKIE D. 2000: Paleooceanographic significance of Late Paleocene dysaerobia at the shelf/slope break around New Zealand. *Palaeogeography, Palaeoclimatology, Palaeoecology* 156, 51–70.
- KING P., NAISH T., BROWNE G., FIELD B. & EDBROOKE S. 1999: Cretaceous to Recent sedimentary patterns in New Zealand. *Institute of Geological and Nuclear Sciences Folio Series* 1. 35 p.
- KURTZ A., KUMP L., ARTHUR M., ZACHOS J. & PAYTAN A. 2003: Early Cenozoic decoupling of the global carbon and sulfur cycles. *Paleoceanography* 18(4), 1090, doi:10.1029/2003PA000908
- LIPPS J. H. 1993: *Fossil prokaryotes and protists*. 342 p., Blackwell Scientific, Boston.
- NIGRINI C. & SANFILIPPO A. 2000: Paleogene radiolarians from Sites 998, 999, and 1001 in the Caribbean. *Proceedings of the Ocean Drilling Program, Scientific Results* 165, 57–81.
- REAY M. 1993: *Geology of the middle part of the Clarence Valley*. Institute of Geological and Nuclear Sciences Geological Map 10. 144 p. + 1 map.
- SANFILIPPO A. & BLOME C. 2001: Biostratigraphic implications of mid-latitude Palaeocene-Eocene radiolarian faunas from Hole 1051A, ODP Leg 171B, Blake Nose, western North Atlantic. In: KROON, D. et al. (Eds.): *Western North Atlantic Palaeogene and Cretaceous palaeoceanography*. Geological Society Special Publication 183, 185–224.
- SANFILIPPO A. & NIGRINI C. 1998a: Upper Paleocene-Lower Eocene deep-sea radiolarian stratigraphy and the Paleocene/Eocene Series boundary. In: AUBRY, M.-P., et al. (Eds.): *Late Paleocene-Early Eocene climatic and biotic events in the marine and terrestrial records*, 244–276, Columbia University Press, New York.
- 1998b: Code numbers for Cenozoic low latitude radiolarian biostratigraphic zones and GPTS conversion tables. *Marine Micropaleontology* 33, 109–156.
- STRONG C., HOLLIS C. & WILSON G. 1995: Foraminiferal, radiolarian, and dinoflagellate biostratigraphy of Late Cretaceous to middle Eocene pelagic sediments (Muzzle Group), Mead Stream, Marlborough, New Zealand. *New Zealand Journal of Geology and Geophysics* 38, 171–209.
- SUTHERLAND R., KING P. & WOOD R. 2001: Tectonic evolution of Cretaceous rift basins in south-eastern Australia and New Zealand: implications for exploration risk assessment. In: HILL K. & BERNECKER T. (Eds.): *Eastern Australasian basins symposium: a refocused energy perspective for the future*. Petroleum Exploration Society of Australia Special Publication 1, 3–13.
- THOMPSON E. & SCHMITZ B. 1997: Barium and the late Paleocene $\delta^{13}\text{C}$ maximum: evidence of increased marine surface productivity. *Paleoceanography* 12, 239–254.
- ZACHOS J., PAGANI M., SLOAN L., THOMAS E. & BILLUPS K. 2001: Trends, rhythms, and aberrations in global climate 65 Ma to present. *Science* 292, 686–693.
- ZACHOS J., WARA M., BOHATY S., DELANEY M., PETRIZZO M., BRILLA., BRALOWER T. & PREMOLI-SILVA I. 2003: A transient rise in tropical sea surface temperature during the Paleocene-Eocene thermal maximum. *Science* 302, 1551–1554.

Manuscript received January 2004

Revision accepted February 2005

Plate 1

Scanning electron micrographs of spumellarian radiolarians from lower Eocene strata, Mead Stream. Scale bars = 100 µm.

1. *Amphisphaera coronata* EHRENBERG gr. CH12076, P30/f534, 176 m, RP8.
2. *Axoprunum* aff. *bispiculum* (POPOFSKY). CH12086, P30/f534, 176 m, RP8.
3. *Axoprunum pierinae* (CLARK AND CAMPBELL). CH12079, P30/f534, 176 m, RP8.
4. *Stylosphaera minor* CLARK AND CAMPBELL. CH12078, P30/f534, 176 m, RP8.
5. *Haliomma* gr. b. (cf. *Theocosphaerella rotunda* (BORISSENKO)). CH12005, P30/f1129, 158.3 m, RP8.
6. *Haliomma* gr. b. CH12001, P30/f1129, 158.3 m, RP8.
7. *Periphaena?* *duplus* (KOZLOVA). CH12020, P30/f1129, 158.3 m, RP8.
8. *Periphaena?* *duplus* (KOZLOVA). CH12019, P30/f1129, 158.3 m, RP8.
9. *Periphaena?* *duplus* (KOZLOVA). CH12016, P30/f1129, 158.3 m, RP8.
10. *Periphaena?* *duplus* (KOZLOVA). CH12018, P30/f1129, 158.3 m, RP8.
11. *Middourium regulare* (BORISSENKO). CH12301, P30/f1129, 158.3 m, RP8.
12. *Monobrachium irregulare* (NISHIMURA). CH12012, P30/f1129, 158.3 m, RP8.
13. *Monobrachium irregulare* (NISHIMURA). CH12011, P30/f1129, 158.3 m, RP8.
14. *Amphicraspedum prolixum* SANFILIPPO AND RIEDEL CH12094, P30/f534, 176 m, RP8.
15. *Amphicraspedum gracilis* (LIPMAN). CH12093, P30/f534, 176 m, RP8.
16. *Amphicraspedum gracilis* (LIPMAN). CH12092, P30/f534, 176 m, RP8.
17. *Amphicraspedum gracilis* (LIPMAN). CH12091, P30/f534, 176 m, RP8.
18. *Amphicraspedum murrayanum* HAECKEL. CH12030, P30/f1129, 158.3 m, RP8.
19. *Amphicraspedum murrayanum* HAECKEL. CH12064, P30/f1129, 158.3 m, RP8.
20. *Amphicraspedum prolixum* SANFILIPPO AND RIEDEL CH12059, P30/f1129, 158.3 m, RP8.
21. *Amphicraspedum prolixum* SANFILIPPO AND RIEDEL CH12089, P30/f534, 176 m, RP8.
22. Spumellarian gen. et sp. indet. CH12085, P30/f534, 176 m, RP8.

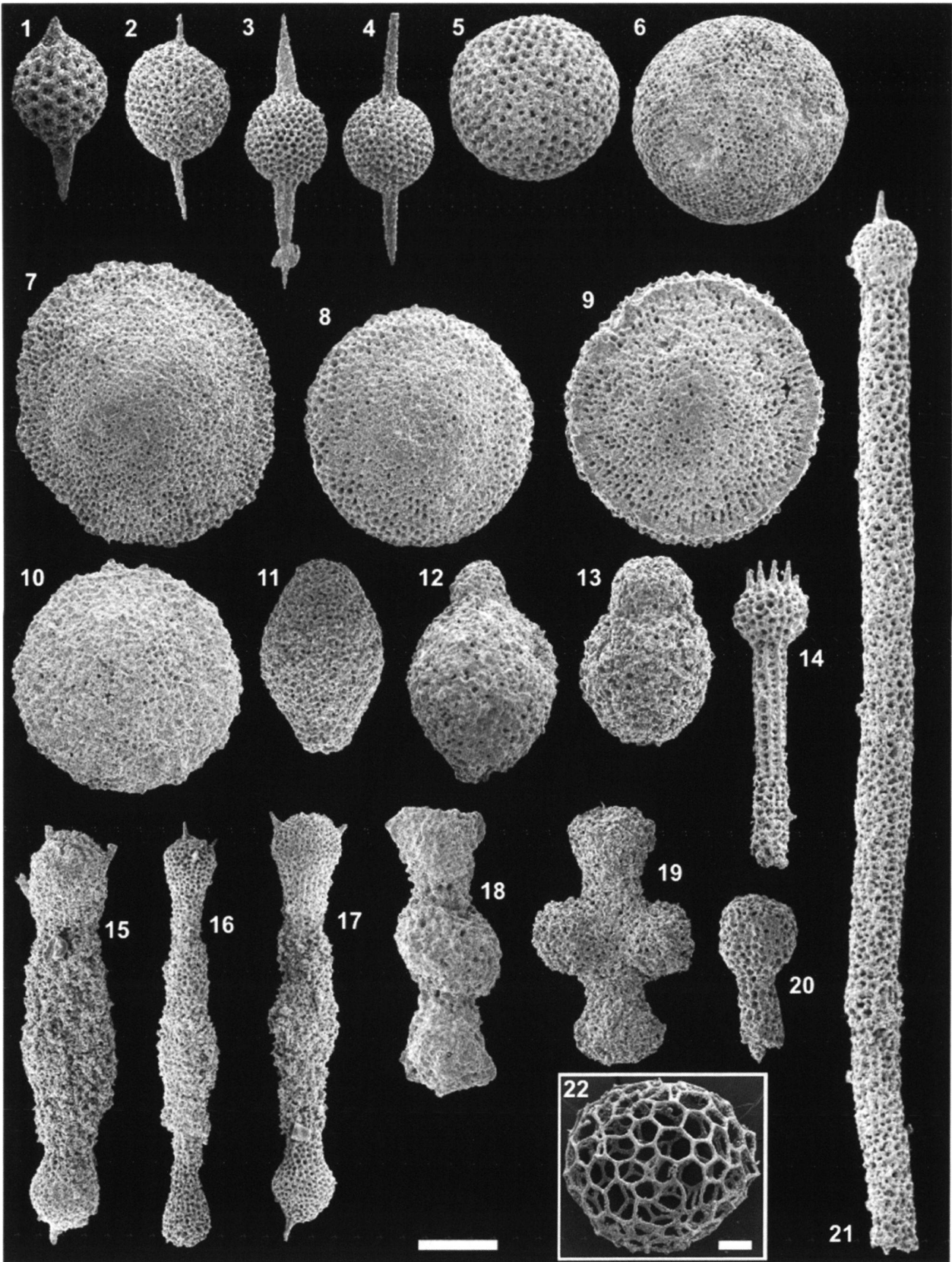


Plate 2

Scanning electron micrographs of nassellarian radiolarians from upper Paleocene (Fig. 4) and lower Eocene strata, Mead Stream.
Scale bar = 100 μ m.

1. *Patagopsyris confluens* (EHRENBERG). CH12074, P30/f1129, 158.3 m, RP8.
2. *Petalospyris foveolata* (EHRENBERG). CH12075, P30/f1129, 158.3 m, RP8.
3. *Clathrocyclus universa* CLARK AND CAMPBELL. CH12103, P30/f534, 176 m, RP8.
4. *Buryella tetradica* FOREMAN. CH01028, P30/f318, 108.3, RP6.
5. *Buryella tetradica* FOREMAN. CH12040, P30/f1129, 158.3 m, RP8.
6. *Buryella tetradica* FOREMAN. CH12065, P30/f1129, 158.3 m, RP8.
7. *Bathropyramis magnifica* (CLARK AND CAMPBELL). CH12101, P30/f534, 176 m, RP8.
8. *Bathropyramis magnifica* (CLARK AND CAMPBELL). CH12100, P30/f534, 176 m, RP8.
9. *Lychnocanium ponderosa* (KOZLOVA). CH12067, P30/f1129, 158.3 m, RP8.
10. *Lychnocanium satelles* (KOZLOVA). CH12098, P30/f534, 176 m, RP8.
11. *Phormocyrtis striata exquisita* (KOZLOVA). CH12070, P30/f1129, 158.3 m, RP8.
12. *Phormocyrtis striata striata* BRANDT. CH12038, P30/f1129, 158.3 m, RP8.
13. *Phormocyrtis turgida* (KRASHENINNIKOV). CH12023, P30/f1129, 158.3 m, RP8.
14. *Phormocyrtis turgida* (KRASHENINNIKOV). CH12056, P30/f1129, 158.3 m, RP8.
15. *Phormocyrtis cubensis* (RIEDEL AND SANFILIPPO). CH12057, P30/f1129, 158.3 m, RP8.
16. *Phormocyrtis cubensis* (RIEDEL AND SANFILIPPO). CH12029, P30/f1129, 158.3 m, RP8.
17. *Phormocyrtis cubensis* (RIEDEL AND SANFILIPPO). CH12028, P30/f1129, 158.3 m, RP8.
18. *Lamptonium fabaeforme fabaeforme* (KRASHENINNIKOV). CH12055, P30/f1129, 158.3 m, RP8.
19. *Lamptonium fabaeforme fabaeforme* (KRASHENINNIKOV). CH12048, P30/f1129, 158.3 m, RP8.
20. *Theocorys? physella* FOREMAN. CH12073, P30/f1129, 158.3 m, RP8.
21. *Theocorys? physella* FOREMAN. CH12042, P30/f1129, 158.3 m, RP8.
22. *Theocorys? physella* Foreman. CH12058, P30/f1129, 158.3 m, RP8.
23. *Theocorys? physella* FOREMAN. CH12045, P30/f1129, 158.3 m, RP8.
24. *Theocorys? physella* FOREMAN. CH12043, P30/f1129, 158.3 m, RP8.

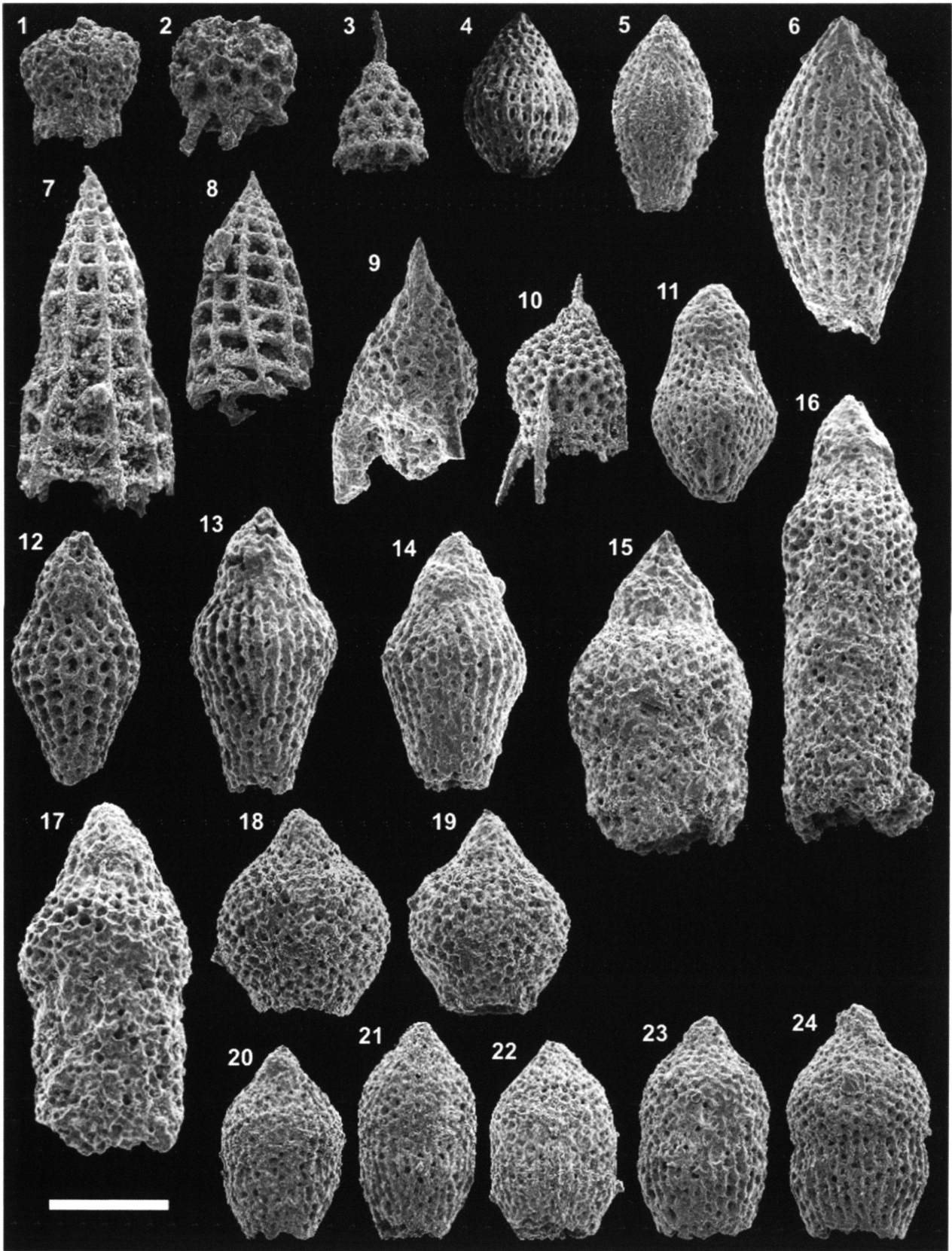


Plate 3

Transmitted light micrographs of radiolarians from upper Paleocene and lower Eocene strata, Mead Stream. Scale bars = 100 μ m.

1. *Haliomma* gr. A-K47/4, P30/f451, 99 m, RP5.
2. *Haliomma* gr. A-L36/3, P30/f533, 166.5 m, RP8.
3. *Haliomma* gr. A-S28/0, P30/f533, 166.5 m, RP8.
4. *Haliomma* gr. A-D29/3, P30/f533, 166.5 m, RP8.
5. *Haliomma* gr. A-R46/1, P30/f533, 166.5 m, RP8.
6. *Periphaena?* *duplus* (KOZLOVA). A-032/2, P30/f451, 99 m, RP5.
7. *Periphaena?* *duplus* (KOZLOVA). A-S31/3, P30/f451, 99 m, RP5.
8. *Periphaena?* *duplus* (KOZLOVA). A-G29/1, P30/f451, 99 m, RP5.
9. *Middourium regulare* (BORISSENKO). A-W53/0, P30/f1076, 136.9 m, RP7.
10. *Dorcadospyris foveolata* (EHRENBERG). A-L49/3, P30/f527, 108.2 m, RP6.
11. *Dorcadospyris foveolata* (EHRENBERG). A-P42/0, P30/f527, 108.2 m, RP6.
12. *Dorcadospyris confluens* (EHRENBERG). A-W50/1, P30/f527, 108.2 m, RP6.
13. *Lophophaena mugaica* (GRIGORJEVA). A-B42/1, P30/f527, 108.2 m, RP6.
14. *Corythomelissa adunca* (SANFILIPPO AND RIEDEL). A-?, P30/f451, 99 m, RP5.
15. *Corythomelissa* sp. A. B-F36/0, P30/f527, 108.2 m, RP6.
16. *Buryella granulata* (PETRUSHEVSKAYA). D-P34/0, P30/f451, 99 m, RP5.
17. *Buryella foremanae* (PETRUSHEVSKAYA). B-U42/0, P30/f527, 108.2 m, RP6.
18. *Buryella tetradica* FOREMAN. A-F48/0, P30/f1076, 136.9 m, RP7.
19. *Buryella tetradica* FOREMAN. D-P32/0, P30/f451, 99 m, RP5.
20. *Buryella pentadica* FOREMAN. C-034/2, P30/f527, 108.2 m, RP6.
21. *Pterocodon poculum* (NISHIMURA). A-O47/2, P30/f1072, 136.6 m, RP7.
22. *Pterocodon poculum* (NISHIMURA). A-L37/3, P30/f1076, 136.9 m, RP7.
23. *Theocorys?* aff. *phyzella* FOREMAN. C-G39/0, P30/f452, 110.8 m, RP6.
24. *Theocorys?* aff. *phyzella* FOREMAN. C-E41/3, P30/f452, 110.8 m, RP6.
25. *Theocorys?* cf. *phyzella* FOREMAN. D-U29/3, P30/f452, 110.8 m, RP6.
26. *Theocorys?* *phyzella* FOREMAN. B-V33/1, P30/f1072, 136.6 m, RP7.
27. *Theocorys?* *phyzella* FOREMAN. A-H34/4, P30/f1072, 136.6 m, RP7.

